Sensors and Materials, Vol. 10, No. 5 (1998) 297–311
MYU Tokyo

S & M 0333

Simultaneous Estimation of Range and Velocity by a Biomimetic Sonar System

Wataru Mitsuhashi

Department of Communications and System Engineering,
The University of Electro-Communications
1-5-1 Chofugaoka, Chofu, Tokyo 182, Japan

(Received October 1,1997; accepted March 23,1998)

Key words: echolocation, Doppler tolerance, bank of constant Q filters, simultaneous estimation of motion parameters

A biomimetic sonar system for simultaneous estimation of the range and the velocity of a moving object is proposed. This system emits linear-period-modulated (LPM) sound that has the time-frequency structure similar to that of echolocation sound utilized by typical echolocating bats. The echoes reflected by objects are processed using a bank of constant-Q (CQ) filters, which mimicks the frequency selectivity in the mammalian auditory periphery. In this system, each filter that composes the CQ filter bank is followed by a number of phase-detecting modules, and each module evokes a pulse in response to a specific phase value of sound stimuli. The ensemble response of all the modules reaches a maximum at a time corresponding to the object's range, and the phase value at the maximum yields information on the object's velocity. The precision in one-dimensional motion measurements performed in air was better than 50 mm/s in velocity and 0.2 mm in range though the LPM sound used in the measurements had a relatively small time-bandwidth product. A conventional sonar system with up-chirp signals did not yield reliable results because of its inherent ambiguity in simultaneous parameter estimation.

1. Introduction

The determination of the locations of moving objects by sound emission, or echolocation, is formulated as a problem of multiparameter estimation. In parameter estimation in radar or sonar applications, an object is represented as a point in a parameter space

characterized by factors such as relative velocity, range, direction, and cross-sectional area. However its image in observation space is blurred by random noise added to the observed signals.[1] This blur is also caused by some dependence among the parameters in the estimation process because they are not necessarily independent of one another. It is therefore desirable that these parameters be independently estimated.

The main parameters to be estimated in radar or sonar applications generally include the range of an unknown object and the relative velocity between the object and the observation platform. With regard to this issue, it has been reported that the use of linear-period modulated (LPM) sound yields accurate estimates of range regardless of the velocity of the object.[2] This kind of sound signal is also known to be emitted as location sound by some species of echolocating bats.[3] In fact, these echolocating bats are known to actively detect and capture certain insects while flying in the dark. These animals have an acute sense for extracting an object's dynamic characteristics, such as velocity, range, direction, and size. This suggests that the study of a biomimetic sonar system is of practical value for reconstructing spatial structures of surroundings by acoustical means.

In a previous study, the author proposed a computational model of echolocation for simultaneous estimation of motion parameters,[4] that is, both the range and the velocity of a moving object. In the proposed model we used LPM sound for echolocation, and a bank of constant-Q (CQ) filters for echo reception, mimicking a typical echolocation sound and the frequency selective response in the mammalian auditory periphery, respectively. After eliminating the group-delay characteristics of the LPM sound, the integration of output waveforms across the filter bank yielded a significant compression of the time duration of the resultant waveforms. This function was equivalent to that of a matched filter composed of dispersive delay lines.

There have been various arguments as to whether a matched filter, or a correlation receiver, exists in bat auditory systems.[5–10] It is generally assumed that a certain kind of biological analog of the correlation operation would exist in the bat auditory system.[5,6] For example, Suga has proposed a neural model for processing range information by cross-correlation analysis.[11] In his model, however, the processing elements for velocity information are composed of frequency-sensitive neurons, and hence, the mechanism for perceiving relative velocity is constructed in a different manner from those for range perception.

In a report of an animal behavioral experiment on the ability of bats to discriminate between a phantom object with phase jitter and a stationary one, Menne *et al.* have suggested that there may exist phase-sensitive mechanisms in the auditory system of the big brown bat, *Eptesicus fuscus*.[12] Saillant *et al.* developed a model of *Eptesicus*' sonar receiver[13] to reconstruct the absolute range and fine range structure of multiple objects from echo spectrograms. In their model, LPM sounds were employed as the sonar sounds of *Eptesicus*, and processed using a bank of filters with tapped delay lines to simulate the coincident detection of phase-locked neural discharges.

In the present study we examine how phase information is important for motion measurement, by developing a mechanism to cast a vote, i.e., to evoke a pulse, in response to a specific phase value of sound stimuli. The resultant histogram of the vote across the bank of CQ filters can be interpreted as the ensemble activity of auditory neurons that

discharge a pulse synchronized with a specific phase of the stimuli. The temporal variation of the histogram will yield a two-dimensional map in which a maximum indicates the existence of an object and the corresponding motion parameters.

In the following sections, a mathematical formulation of motion estimation by sound emission, a design of location sounds, and a brief outline of the mechanism of obtaining motion information are presented. Experimental results of motion estimation performed in air in a one-dimensional environment are presented in comparison with conventional correlation detection of linear up-chirp sounds.

2. Acoustical Measurement of Object Motion

Acoustical measurement to determine the exact location of objects is a fundamental way of reconstructing spatial structures in invisible environments, and has been used in a variety of applications. For motion measurements, however, the Doppler effect must be taken into careful consideration because of the relatively slow speed of sound propagation. Since the Doppler effect is theoretically formulated as the temporal dilation of echo waveforms,[14] the time-frequency structures of echoes reflected by moving objects will generally vary from those of emitted sounds. For the precise estimation of the range and the velocity, it is therefore important to design a sound to be immune to the Doppler effect.

Let us consider the case where a transmitter emits an echolocation sound $u(t)$ and a receiver detects the echo $e(t)$ reflected at a range r_o by a pointlike object moving with a constant velocity v_o. If the sound $u(t)$ has a relatively long duration, the position of the reflection from the moving object is different for each temporal component of the sound. Thus, the distance of travel of each of the components differs. In consideration of this condition, Kelly and Wishner have derived the following equation for a generalized representation of the echo reflected from an object moving with constant velocity:

$$e(t) = \sqrt{s_o} \cdot u\left(s_o \cdot (t - \tau_o)\right), \tag{1}$$

where τ_o denotes the round-trip delay time of sound propagation between sound emission and the corresponding echo reception, and s_o the temporal dilation due to the Doppler effect caused by the object's motion relative to the observation platform.[14] It is assumed in this formulation that the signal component at the time origin, $u(0)$, is reflected by the object just at $\tau_o/2$. However, this assumption does not necessarily mean that $u(t)$ must have energy at $t = 0$. If the range from the transmitter to the object at the time of reflection is exactly r_o, the following relationships hold:

$$\tau_o = \frac{2r_o}{c} \quad \text{and} \quad s_o = \frac{c - v_o}{c + v_o}, \tag{2}$$

where c is the velocity of sound.

The estimation of the range and the velocity of a moving object is thus accomplished by the measurement of the following two parameters: the round-trip delay time τ_o and the dilation factor s_o. However, if the object's velocity is unknown, then it is difficult to estimate the object's range at an arbitrary time. Equation (2) implies that the measurement of τ_o yields only the range r_o at the time of reflection. This difficulty is fairly serious when there exist many objects to be measured. In the case of flow-field measurements, for example, various objects at different ranges are moving with different velocities, and reflections of the sound from these objects do not occur at the same time. In this situation, as long as we depend only on delay measurement, we cannot determine the ranges to the places where individual objects simultaneously exist. However, this uncertainty can be solved if all object velocities are known.

Suppose that r_e, shown in Fig. 1, denotes the range of an object from the observation platform when sound emission has just started, i.e., when $t = 0$. If the object moves along the line of sight with velocity v_o, the range r_o at the time of reflection does not agree with r_e, and the difference between these ranges increases linearly with the object's velocity:

$$r_o - r_e = v_o \cdot \frac{\tau_o}{2}. \tag{3}$$

However, from eqs. (2) and (3), the range of a moving object at the time of sound emission is indirectly expressed as

$$r_e = \tau_o \cdot \frac{c - v_o}{2}, \tag{4}$$

so that we can determine the range of each object at $t = 0$, if both τ_o and v_o can be estimated independently.

Having examined the uncertainty in motion measurements, we now consider, in the next section, how to resolve this problem by adopting a biomimetic sonar system.

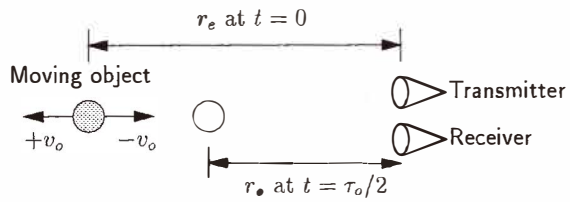

Fig. 1. Uncertainty in range measurement. When an object is moving, the position at the time of sound reflection differs due to the object's velocity. Thus, in the case of multiple objects moving with various velocities, the round-trip delay measurement without velocity information does not provide the positions where these objects simultaneously exist.

3. Design of Location Sound and Receiver for Motion Parameter Estimation

Since an echo reflected by a small object is usually buried in environmental noise, a correlation detector is used as a receiver to detect the existence of the echo. However, as shown in eq. (1), the time-frequency structure of the echo $e(t)$ differs from that of the emitted sound $u(t)$ because of temporal dilation caused by the Doppler effect. Thus, the correlation between $e(t)$ and $u(t)$ will degrade depending on the object motion. For this reason, we must design a sound $u(t)$ that has a property independant of the Doppler effect.

3.1 *Linear-period-modulated sound*

Kroszczynski investigated a frequency modulation law for Doppler invariance, and derived an optimum signal in an analytic form to minimize signal degradation resulting from Doppler distortion:[2]

$$u(t) = a(t) \cdot \exp\left\{ j\left(\Omega \ln t + \Omega_0\right)\right\}, \; t > 0, \tag{5}$$

where Ω and Ω_0 are arbitrary real variables for determining the time-frequency structure of the signal, and $a(t)$ denotes an envelope function. If the envelope $a(t)$ varies slowly in time compared with the temporal change of the phase $\Omega \ln t$, the instantaneous frequency of $u(t)$ is given by the time derivative of its phase as

$$\omega = \frac{d\left(\Omega \ln t + \Omega_0\right)}{dt} = \frac{\Omega}{t}. \tag{6}$$

Equation (6) shows that the instantaneous period of this signal increases linearly with time, and accordingly, this type of signal formulation is called '*linear-period modulation* (LPM).'[2,15] It has been pointed out that the LPM sound has the features typical of the FM location sounds produced by the little brown bat *Myotis lucifugus*.[3]

Substituting eq. (5) into eq. (1) yields

$$\begin{aligned} e(t) &= \sqrt{s_0}\, a\left(s_0 \cdot \left[t - \tau_0\right]\right) \cdot \exp\left\{ j\left(\Omega \ln\left(s_0 \cdot \left[t - \tau_0\right]\right) + \Omega_0\right)\right\} \\ &\cong \exp\left(j\Omega \ln s_0\right) \cdot u\left(t - \tau_0\right), \end{aligned} \tag{7}$$

which results from the approximation $\sqrt{s_0} \cong 1$, and from the assumption that the effect of temporal dilation on the envelope $a(t)$ can be negligible. Since the echo $e(t)$ in eq. (7) is a translated and phase-rotated version of the emitted sound $u(t)$, the cross-correlation function of $e(t)$ with $u(t)$ can be represented by the autocorrelation function of $u(t)$ with an additional phase:

$$\phi_{eu}(\tau) = \exp(j\Omega \ln s_o)\phi_{uu}(\tau - \tau_o). \tag{8}$$

Since the autocorrelation function $\phi_{uu}(\tau)$ has the maximum at $\tau = 0$, the envelope of the cross-correlation function $\phi_{eu}(\tau)$ also peaks at $\tau = \tau_o$ without any influence of the Doppler dilation s_o. If the velocity is much slower than that of sound propagation, we have an approximation of the phase in eq. (8) such that

$$\varphi_o = \Omega \ln s_o \cong \Omega \ln(1 - 2v_o / c) \cong -\Omega \cdot (2v_o / c). \tag{9}$$

Therefore, Doppler-invariant range estimates can be obtained by finding the time of the maximum, τ_o, as can velocity estimates by examining the corresponding phase, φ_o, at τ_o.

3.2 *Bank of constant-Q filters alternative to a correlation receiver*

The maximum amplitude mentioned above is due to the fact that individual frequency components of the sound $u(t)$ are aligned in phase at τ_o. The time when all of the frequency components are in phase will thus yield an important clue to range estimation. Thus, we can realize a function equivalent to the correlation operation by decomposing the sound $u(t)$ into various frequency components, canceling the group-delay characteristics of the sound, and then integrating all the frequency components to a single output waveform. Figure 2 shows a bank of filters followed by time-delay devices for group-delay cancella-

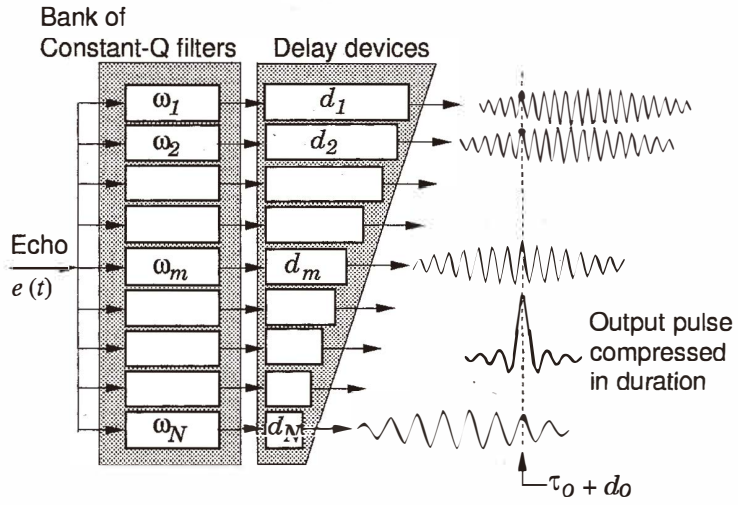

Fig. 2. A conventional scheme of pulse compression by means of the "delay & sum" process. A bank of filters, followed by appropriately designed delay devices, provides a function equivalent to that of a correlation receiver.

tion. A quadrature implementation of each filter will provide a function equivalent to that of a coherent correlation receiver. However, as shown previously in eqs. (7) and (9), the phase at τ_o will also provide information on an object's velocity. In the present study, therefore, we will exploit a system which examines the temporal variation of the phase distribution across the filter bank, as an alternative means of integrating the output of each filter. The phase of the filter output can be easily calculated if the filter has mutually orthogonal components for its real and imaginary parts.

Let t_m be the time when the phase of the LPM signal in eq. (5) becomes an integer m multiple of 2π radians:

$$\Omega \ln t_m + \Omega_o = 2\pi \times m. \tag{10}$$

Based on eq. (6), we represent the instantaneous frequency at t_m by

$$\omega_m = \frac{\Omega}{t_m}. \tag{11}$$

Using eqs. (10) and (11), we obtain the following relationship between those instantaneous frequencies adjacent to each other:

$$\ln \omega_{m+1} - \ln \omega_m = \frac{2\pi}{\Omega}. \tag{12}$$

Thus, for each m, ω_m takes a value at equal intervals on the logarithmic frequency axis, as shown in Fig. 3. This figure also illustrates the underlying concept for determining both the center frequency of each filter and the corresponding amount by which to cancel the group delay such that

$$d_m = d_o - \frac{\Omega + 2Q}{\omega_m}, \tag{13}$$

where d_o is required to satisfy the causality and Q denotes the Q value common to all CQ filters.[4] In eq. (13), Ω/ω_m represents the group delay of the LPM sound at the frequency of ω_m, and $2Q/\omega_m$ is that of the filter tuned to ω_m.

If each filter is connected with a delay device to cancel the group-delay characteristics, then the outputs of all the filters will have the same value of phase at a certain time corresponding to echo reception. In Fig. 4 the temporal variation of the phase of the filter tuned to ω_m is represented by the line whose inclination with respect to time is ω_m. These lines will eventually intersect at a specific time, $\tau_o + d_o$. Again, this intersection arises from the fact that all the outputs have the same value of phase, $\varphi_o = -\Omega \cdot (2v_o/c)$, exactly at time $\tau_o + d_o$. Since the output signals are processed in digital form, the phase is also sampled at discrete intervals of Δt, as shown by the open circles along those lines illustrated in Fig. 4. The resultant histogram of the circles in time and phase dimensions can be interpreted as a

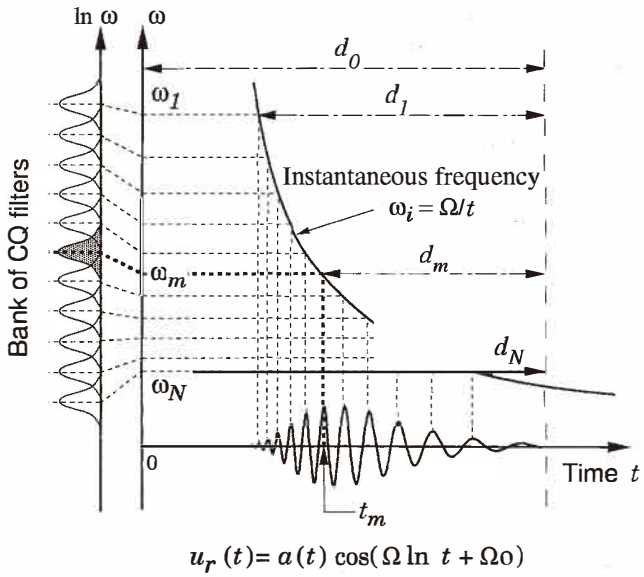

Fig. 3. Instantaneous frequency characteristics of the emitted LPM sound. The frequency increases linearly on the logarithmic scale as the phase of the LPM sound rotates. A bank of constant-Q filters is thus constructed on the basis of the frequencies corresponding to those values of phase at regular intervals.

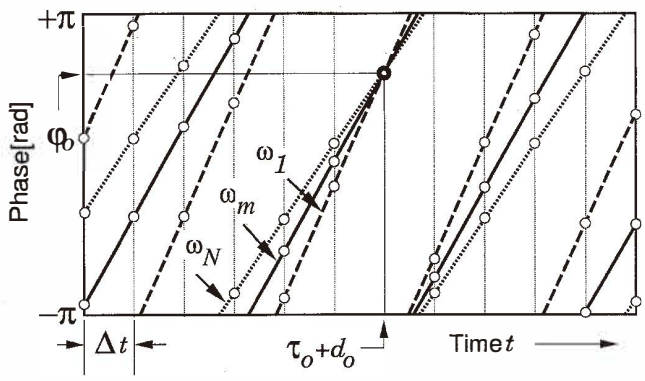

Fig. 4. Trajectories of phase evolutions of output signals from individual filters. Since the slope of a trajectory depends on the center frequency of the corresponding filter, these trajectories eventually intersect each other. The position of the intersection will provide information relevant to object motion.

probability distribution associated with an object's motion in the delay-Doppler domain. That is, the position of a dominant peak in the histogram provides the range and the velocity estimates for the corresponding object.

4. Results and Discussions

Experiments for motion estimation were carried out in air. The mean air temperature was 15.5°C and the speed of sound therefore was about 341 m/s. Polyvinylidene fluoride (PVDF) films resonant at a frequency of 50 kHz were used as a speaker and a microphone, for transmission and reception of location sounds, respectively. For the LPM sound, we determined Ω and Ω_o in eq. (5) such that

$$\Omega = c\pi, \quad \Omega_o = 0. \tag{14}$$

Under this condition, the phase rotation $2\nu_o\Omega/c$ in eq. (9) becomes π at the relative velocity of ν_o = 500 mm/s; therefore, velocity estimation by the measurement of phase rotation was limited to within ± 500 mm/s. In accordance with the frequency characteristics of the PVDF films, the frequency of the LPM sound was swept downward hyperbolically from 60 kHz to 40 kHz within the duration of about 1.42 ms. To compare the performance of parameter estimation, we also used a linear up-chirp sound with the same time-bandwidth product as that of the LPM sound. The instantaneous frequency characteristics of these two sounds are illustrated in Fig. 5.

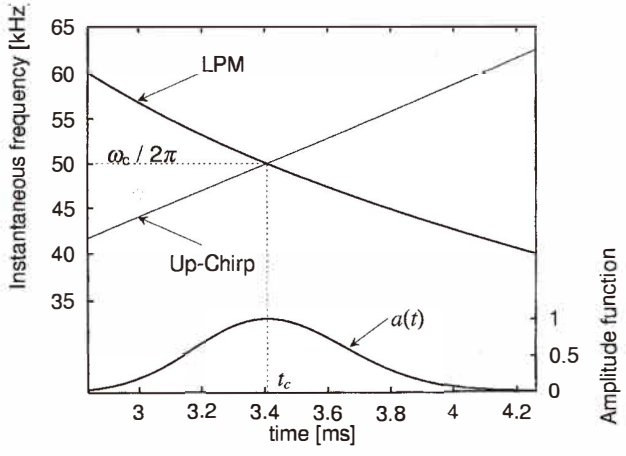

Fig. 5. Two different types of echolocation sounds with the same time-bandwidth product. The amplitude function is common to these two location sounds used.

Figure 6 illustrates the experimental setup for 1D motion measurement. The object used in the experiments was a plastic disk of 20 mm diameter driven along the line of sight of the transducers. The velocity of the object was precisely controlled from −400 mm/s to +400 mm/s in 40 mm/s steps by varying the frequency supplied to a stepping motor. However, a slight fluctuation in the velocity was unavoidable because of mechanical wear or friction.

In order to detect the passage of the object and provide the origin of the time axis, we used a photosensor; when the object passed the sensor, the speaker was immediately triggered to emit one of the location sounds. The range from the sensor to the transducer mount was measured to be about 1,000 mm using a standard rule for industrial use. The actual range is expected to be shorter than this value because the vibrating plate of the transducers is curved cylindrically outward.

The echo reflected from the object was received by the microphone, and digitized by means of an analog-to-digital converter sampling at every 2 μs with 12-bit resolution. The emitted LPM sound and a typical example of echo waveforms are plotted in Fig. 7.

After DC offset and noise components were removed by numerical operation, the echo was applied either to the bank of CQ filters designed for the LPM sound to produce the histogram in the delay-Doppler domain, or to the correlation detector for the chirp sound to produce pulse-compressed outputs. In the case of the LPM sound, we can determine the range and the velocity estimates by seeking a dominant peak in the histogram and finding its coordinates. In contrast, for the chirp sound, we must usually prepare a large number of correlation detectors and various hypothesized references to perform a maximum likelihood decision of motion parameters; the hypothesized reference yielding the highest correlation provides an estimate of the parameters of object motion. To compare the performance of parameter estimation, however, we simply used a single correlation detector in which the hypothesized velocity was set to 0 mm/s, so that biased estimates in the range estimation were unavoidable.

The CQ filter bank was composed of 60 constant-Q, 2nd-order IIR filters with $Q = 15\pi$. A similar performance of motion parameter estimation was found for Q values from 10π to 20π. Typical examples of the histogram in the delay-Doppler domain are illustrated in Fig.

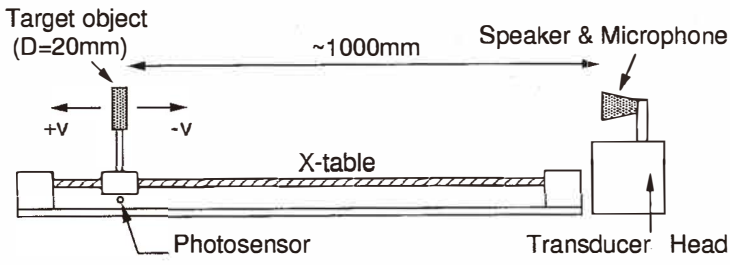

Fig. 6. Experimental setup for one-dimensional motion measurements. Upon detecting the passage of the object, the photosensor immediately triggers the emission of echolocation sounds.

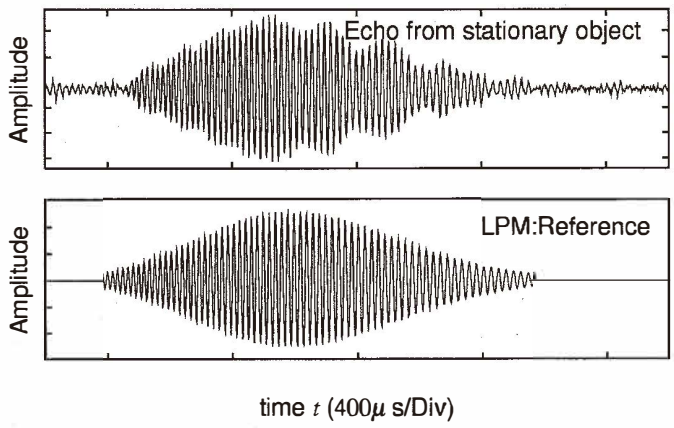

Fig. 7. A typical example of echoes reflected by the object used (upper) and the emitted LPM sound (lower). Both ordinates are arbitrarily scaled.

8. As shown in this figure the histogram consists of inclined ridges, so that an error along the delay axis, $\delta\tau$, inevitably results in the corresponding error along the Doppler axis such that

$$\delta\varphi = \omega_C \cdot \delta\tau, \tag{15}$$

where ω_C is the mean inclination of these ridges and is equivalent to the center frequency calculated from the first-order spectral moment of the LPM sound. Since the velocity is estimated by the relation $v_o = -\varphi_o/2\pi$ from eqs. (9) and (14), and the range by $r_o = c \cdot \tau_o/2$ from eq. (2), the velocity estimates are not independent of the range estimates, and error in velocity estimation, δv, can be associated with the range error δr as

$$\frac{\delta v}{\delta r} = -\frac{1}{c\pi} \cdot \frac{\delta\varphi}{\delta\tau} = -\frac{\omega_C}{c\pi}. \tag{16}$$

In the case where c = 341 m/s and $\omega_C \sim 2\pi \times 50$ kHz, $\delta v/\delta r$ will become about -293 1/s. To confirm this relation, a set of 20 emissions of the LPM sound was directed at a stationary object that was placed about 1 mm away from the photosensor. Since the object was stationary, thermal noise and variations in the propagation medium between the object and the transducers would mainly result in a fluctuation of the position of the maximum in the histogram. Velocity estimates observed in this trial are plotted in Fig. 9 against the corresponding range estimates. Several outliers shown in this plot are presumed to occur as a result of timing jitter in the data acquisition system used. Most of these estimates, excepting the outliers, are linearly distributed along a line having a slope of -288 1/s. This

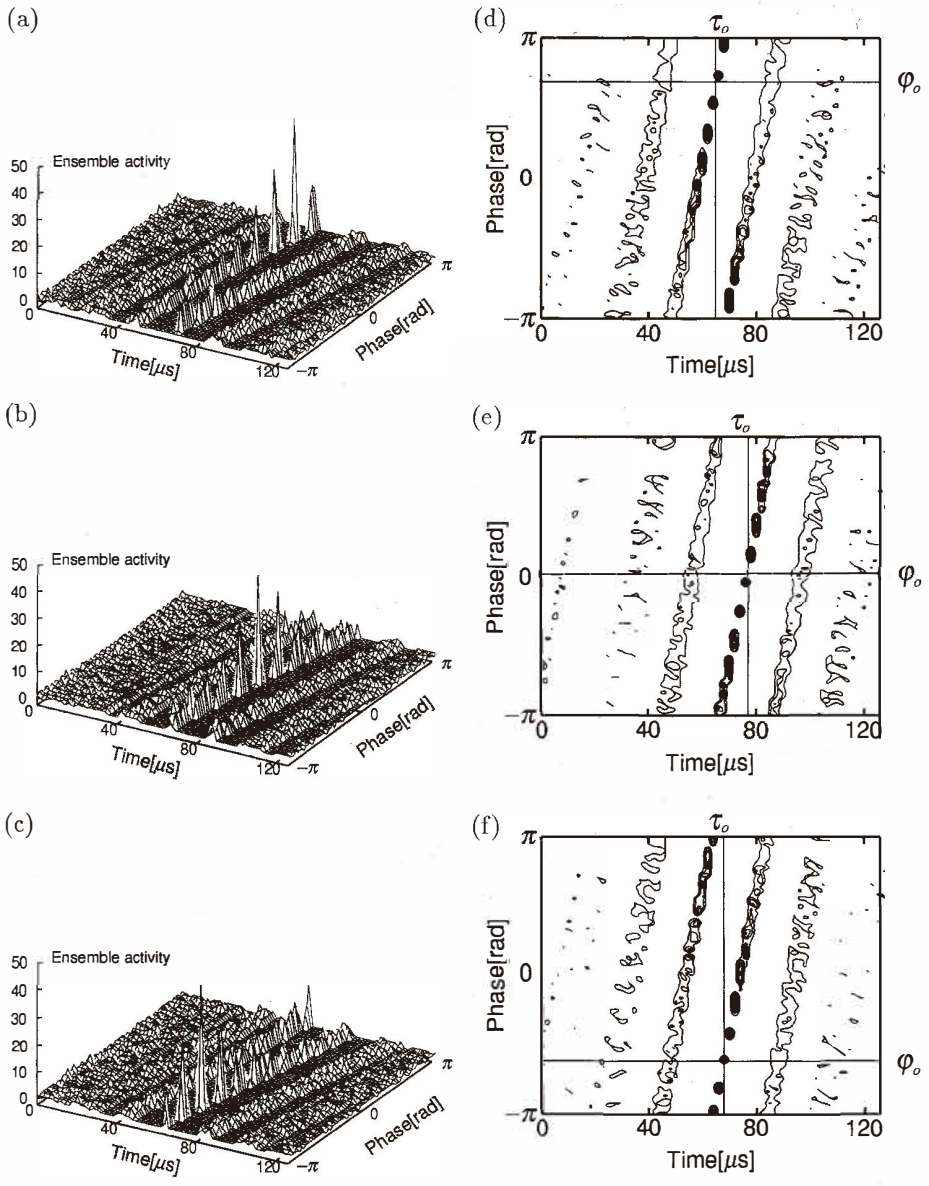

Fig. 8. Perspective views (a, b, c) and contour plots (d, e, f) of ensemble activities of phase-detecting modules connected to the CQ filter bank. The histogram of the ensemble activity yields information relevant to object motion. For example, one can determine, from (a) and (d), that the object is approaching the transducers because the phase of the dominant peak has a positive value (the reader may refer to eq. (9) in section 3).

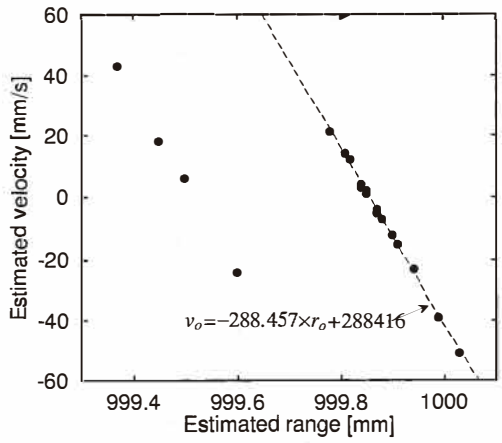

Fig. 9. Fluctuations of range and velocity estimates due to environmental noise. Several outliers are presumed to occur as a result of timing jitter in the data acquisition system used in the experiment. The dashed line obtaind by linear regression shows that the fluctuations of these estimates can be represented as $\delta v = -288 \times \delta r$. A slight bias in velocity estimates can also be observed.

value agrees well with the theoretical relation derived above. Figure 9 also indicates that these estimates are scattered around its center within the range of about ±0.13 mm in range and ±36 mm/s in velocity; the velocity estimates are slightly negatively biased. The distribution of these estimates shows the basic behavior of our bionic sonar system under environmental noise.

After confirming the behavior of our system against random noise, we finally carried out motion measurements by driving the object at different velocities along the line of sight of the transducers. Figure 10 shows an example of velocity estimates derived by determining the coordinates of the dominant peak of the histogram in the delay-Doppler domain. It can be seen that the velocity estimates are negatively biased, as expected from the result shown in Fig. 9. This biased amount can be removed in advance by introducing an offset in the phase determination. The standard deviation from the values expected based on line-fitting to the velocity estimates was about 40 mm/s.

The range estimates r_e at $t = 0$ derived from eq. (4) are shown in Fig. 11, along with the results estimated by correlation detection for the chirp sound. Discontinuities in the range estimates at $v = 0$ in Fig. 11 arise because the photosensor had a finite width of the receptive area that detects the passage of an object; that is, the timing of sound emission differed according to whether the object approached (i.e., $v_o < 0$), or receded ($v_o > 0$) from the transducers. The mean value of the range estimates when $v_o > 0$, was 996.5 mm and when $v_o < 0$, was 997.4 mm. The difference between these mean values can be attributed to the size of the receptive area of the photosensor. The standard deviation was about 0.14 mm for both directions of object motion.

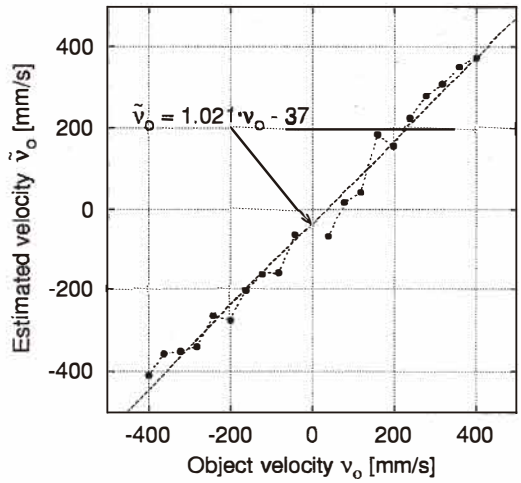

Fig. 10. Velocity estimates (connected black circles) plotted vs actual velocity. A slightly biased amount in the velocity estimates appears to correspond to the bias observed in Fig. 9.

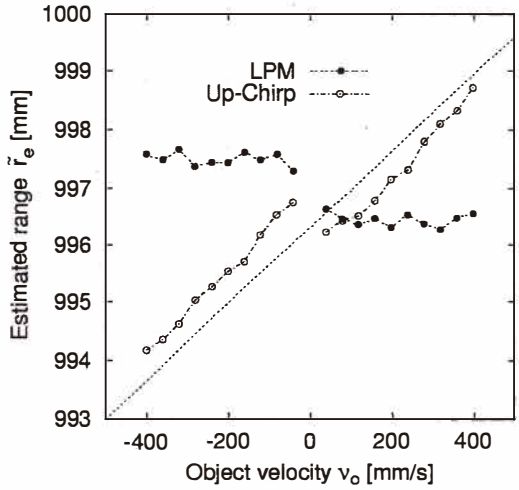

Fig. 11. Corrected range estimates r_e. Ambiguous property still remains in the range estimates obtained using the up-chirp sound. The dotted line indicates the theoretical ambiguity for the chirp sound in range estimation.

For the chirp sound processed by a single correlation detector we cannot estimate the object range precisely as long as the object velocity is unknown. Hence the range estimates for the chirp sounds shown in Fig. 11 were calculated using the actual object velocity as a hypothesized reference for each trial. An ambiguous property of chirp sounds in motion parameter estimation[16] still remains in Fig. 11. The dotted diagonal line in this figure shows the theoretical ambiguity for the up-chirp sound used in the experiments.

5. Summary

Simultaneous estimation of motion parameters can be performed using a biologically based system, without a correlation operation. The parallel connections of CQ filters and the construction of histograms in the delay-Doppler domain are suited to real-time operation. Regardless of the relatively small time-bandwidth product of the LPM sound used, the precision in 1D estimation was better than 50 mm/s for velocity and 0.2 mm for range. In contrast, the sonar system using up-chirp sound did not yield reliable results because of the ambiguous property in parameter estimation.

Acknowledgment

This research was supported by the Ministry of Education, Science, Sports and Culture, Japan, under a Grant-in-Aid for Scientific Research (C)06650456 and (B)09450172.

References

1 H. L. Van Trees: Detection, Estimation, and Modulation Theory, Part I (John Wiley, New York, 1968) Chap. 2.
2 J. J. Kroszczynski: Pulse compression by means of linear-period modulation, Proc. IEEE **57** (1969) p. 1260.
3 R. A. Altes and E. L. Titlebaum: J. Acoust. Soc. Am. **48** (1970) 1014.
4 W. Mitsuhashi: "Echo location systems," Intelligent Sensors, ed. H. Yamasaki (Elsevier Science B.V., Amsterdam, 1996) p. 191.
5 J. A. Simmons: J. Acoust. Soc. Am. **54** (1973) 157.
6 J. A. Simmons: Science **204** (1979) 1336.
7 G. Neuweiler: Physics Today (August 1980) 34.
8 D. Menne and H. Hackbarth: J. Acoust. Soc. Am. **79** (1986) 386.
9 B. Møhl: Acustica **61** (1986) 75.
10 H. Hackbarth: Biol. Cybern. **54** (1986) 281.
11 N. Suga: Neural Networks **3** (1990) 3.
12 D. Menne, I. Kaipf, I. Wagner, J. Ostwald and H. -U. Schnitzler: J. Acoust. Soc. Am. **85** (1989) 2642.
13 P. A. Saillant, J. A. Simmons, S. P. Dear and T. A. McMullen: J. Acoust. Soc. Am. **94** (1993) 2691.
14 E. J. Kelly and D. P. Wishner: IEEE Trans. Military Electron. **MIL-9** (1965) 56.
15 R. A. Altes and D. P. Skinner: J. Acoust. Soc. Am. **61** (1977) 1019.
16 C. E. Cook and B. Bernfeld: Radar Signal (Academic Press, New York, 1967) Chap. 6.